Operational limits on WEST inertial divertor sector during the early phase experiment

M. Firdaouss[a], Y. Corre[a], P. Languille[a], H. Greuner[b], E. Autissier[a], C. Desgranges[a], D. Guilhem[a], J. P. Gunn[a], M. Lipa[a], M. Missirlian[a], J.-Y. Pascal[a], C. Pocheau[a], M. Richou[a], E. Tsitrone[a]

a CEA, IRFM, F-13108 Saint-Paul-Lez-Durance, France

b Max-Planck-Institut for Plasma Physics, Boltzmannstr. 2, 85748 Garching, Germany

E-mail: mehdi.firdaouss@cea.fr

Abstract

The primary goal of the WEST project is to be a test-bed to characterize fatigue and lifetime of ITER-like W divertor components subjected to relevant thermal loads. During the first phase of exploitation (S2 2016), these components (W monoblock plasma facing unit - W-PFU) will be installed in conjunction with graphite components (G-PFU). As the G-PFU will not be actively cooled, it is necessary to ensure that the foreseen pulse duration allows for the W PFU to reach their steady-state without overheating the G-PFU assembly structure or the embedded stainless steel diagnostics. High heat flux test have been performed at the GLADIS facility to assess the thermal behaviour of the G-PFU. Finally, some operational limit depending on plasma parameters are determined. It is shown that it is possible to operate at an injected power such that the maximal incident heat flux on the lower divertor is 10MW/m² for the required pulse length.

1. Introduction

The main objective of the WEST (W Environment in Steady-state Tokamak) project, which is an upgrade of the Tore Supra limiter machine, is to fabricate and test an ITER-like actively cooled tungsten divertor made of 456 W-PFU, in order to reduce the manufacturing and divertor operation risks for ITER. Therefore the magnetic X-point configuration (lower single null, upper single null or double null) will be created by the installation of divertor coils inside the vacuum vessel. Plasma facing components (PFC) comprising the upper divertor and baffle are W-coated actively cooled components with a CuCrZr based heat sink. The W-PFU should withstand heat fluxes close to 10MW/m², which is expected during ITER normal operation and even 20MW/m² during slow transients [1]. It is therefore necessary to verify that for those levels of power the remaining PFCs are not overloaded.

Three different designs of the lower divertor target, composed of 12 sectors of 38 PFU each are already foreseen because of delays in production of the W-PFU. The first version to be installed will be made of non-actively cooled graphite components with a thin W coating (< 15µm). The second version will be made of actively cooled CuCrZr components also with thin W coatings. Then it will be progressively replaced by the third version made of W monoblocks bonded to a copper alloy tube (ITER-like W-PFU). It is important to note that all those three types of PFU will have an identical surface exposed to the plasma, meaning that the same scenario will produce the same heat flux on any of them. The difference will be in the capability of the G-PFU to endure a high level heat load during long pulses.

The goal of this paper is to analyse the operational limitations attributed to the graphite inertial sectors and discuss the consequences for the scientific exploitation of WEST during the early operation phase. The operational limitations on this PFU are due to the combination of different kinds of issues: damage of the G-PFU attachment to the support, melting of the embedded stainless steel diagnostics and delamination of the coating interface. The first two cases were carefully analysed during the design phase with finite elements simulations, which is reported in the first section. The assumptions made during the design phase were tested with dedicated high heat flux experiments at GLADIS neutral beam facility [2]. These results are presented in the second section. Finally, we discuss the coating limits (already known from past experiments) compared to the limits defined in the previous section. The main limit depends on the scenario: for high power/short pulses, the limit is driven by the coating (due to the high surface temperature) while for low power/long pulses it is driven by the stainless steel diagnostics (due to diffusion of heat into the bulk of the PFU). Nevertheless it is possible to operate with a maximal incident heat flux of 10 MW/m² on the lower divertor during the required duration without risking the integrity of the G PFU.

2. Mechanical attachment optimization and localization definition of the embedded diagnostics

As mentioned previously the G-PFUs installed on the lower divertor during the first exploitation phase are made of graphite. 13 different types of G-PFU are planned. They are then assembled in 30° sectors of 38 (standard sector) or 36 (sector with Langmuir probes) G-PFU. Each individual G-PFU is poloidally divided in two parts, high field side (HFS) and the low field side (LFS) PFU (see Fig. 1). The gap between those two G-PFU is in the private flux region below the X-point for the foreseen plasma configuration ([3]). Both of LFS and HFS PFU are shaped. The other types of G-PFU are mainly equipped with embedded diagnostics such as thermocouples (TC - up to 1100°C) and fiber Bragg grating (FBG - up to 1200°C) for measuring the temperature and Langmuir Probes (LP) for measuring some plasma physical properties. The PFU with LP are 1.5 times larger than the standard elements, to provide sufficient volume to house the probes without weakening the G-PFU, and space to lay the 58 coaxial cables used to power the probes.

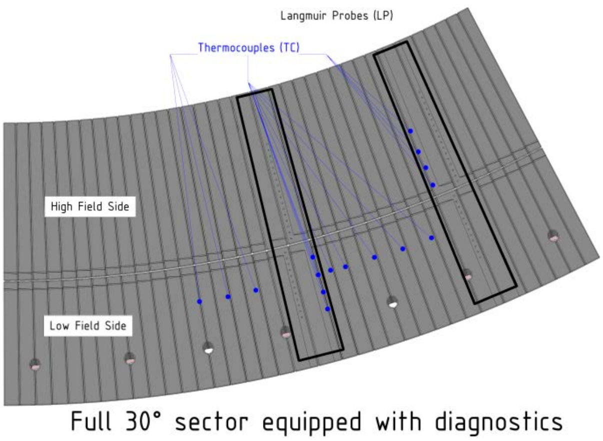

Figure 1: 30° sector of 36 PFU equipped with 58 Langmuir Probes and 16 thermocouples

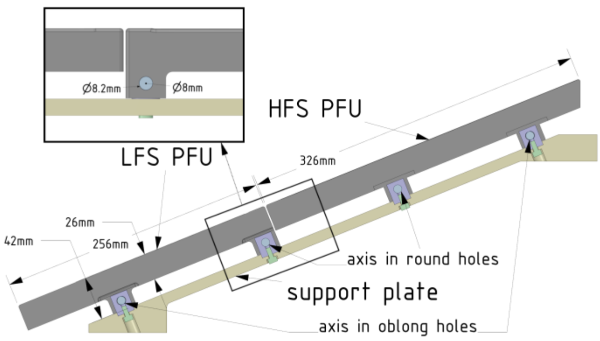

Figure 2: Side view of the LFS and HFS PFU with their attachment to the support plate

The material used for the best compatibility in terms of coefficient of thermal expansion with the W coating is the graphite R6710 from SGL, the same as used in the ASDEX Upgrade divertor [4, 5]. However this material exhibits a brittle behaviour and has a low ultimate strength, typically 170 MPa for a compressive stress and 50 MPa for a tensile stress. For that reason the G-PFU are linked to their support with a mobile attachment (see Fig. 2): on one extremity the hole containing the pin is round; on the other it is oblong to accommodate thermal expansion. However it is necessary to ensure that the stress in this area is below the design limit.

The limitations originating from the coating are well known, since the same coating has been used for JET ITER-like Wall and ASDEX Upgrade [4, 5]. In general, the W coating (including a Mo inter-layer) has shown its capability to sustain temperature up to 1800°C for at least 100 cycles without delamination. However, this conclusion depends greatly of the total heating time. Indeed, it is clearly shown [5] that the carbidisation of the Mo and W which occurs above 1200°C, greatly weakens the coating. Therefore it is foreseen to limit the surface temperature of the G-PFU to 1200°C for the standard operation, but to allow to go further for a limited number of dedicated experiment, for example up to 1600°C to 1800°C.

2.1 Stress at the attachment interface

In a first design stage, the bore for the axis in the graphite is 8mm, the same size than the axis. Finite element simulations have been performed with the ANSYS code. The thermal load is chosen in the PFCFlux-code simulations [3] from available assumptions to maximize the thermal energy and therefore the mechanical stress: 5MW/m² (peaked) during 15s, followed by 1000s of cooling by radiation in close X-point plasma configuration with a decay length (lq) of 5mm (important spreading of the heat flux).

The maximal surface temperature after 15s is 1700°C. After 1000s for the cooling phase, the temperature is homogeneous in the PFU at 250°C. The maximal tensile stress has been calculated during both heating and cooling phases, especially near the attachment axis. The size of the hole is optimized in order to minimize the tensile stress, which has to be lower than 13MPa (ultimate tensile strength of 50MPa with a margin ratio of 4).

Max tensile stress (MPa)	15s		1000s	
Ø hole	Axis	Bulk	Axis	Bulk
8mm	30	40	80	15
8.1mm	2	15	10	0.5
8.2mm	1	12	5	0.2

Table 1: Evolution of the calculated maximal tensile stress in the PFU at the end of heating (15s) and cooling (1000s) phases, for different hole diameters, near the attachment axis and in the bulk material.

It is clear from the results presented in the table 1 that holes with dimensions too close to the nominal diameter of the axis could be very damageable to the PFU. The chosen diameter is 8.2mm, which allows a compatible tensile strength while ensuring a reasonable attachment clearance.

2.2 Temperature field near the diagnostics.

Under the same conditions, the position of the diagnostics has been verified in order to ensure an acceptable temperature range for the instrumentation. The TC are planned to be installed 7.5mm underneath the incident surface, the FBG 4mm and 7.5mm. The screwing support of the LP will be located 20mm below the surface.

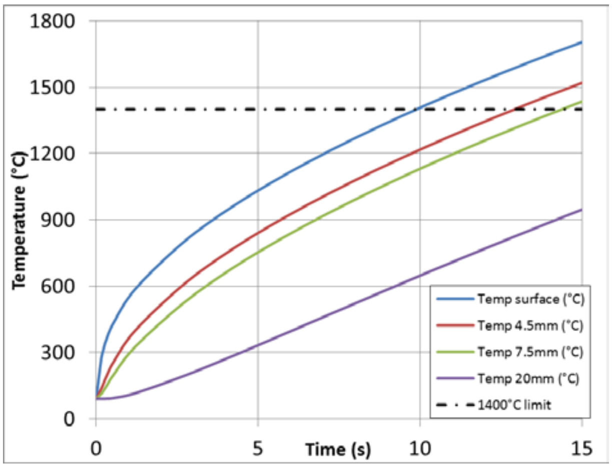

Figure 3: Temperature in the PFU at different depth as a function of time for 5MW/m² during 15s

The initial design of the LP fixation scheme and the sheaths of the TC and FBG are in stainless steel, whose melting point is around 1400°C (dashed line on figure 3). From figure 3 it is clear that at the end of the heat flux pulse the graphite near the TC and FBG will be at a higher temperature than the melting point of the steel for this conservative case. However, the melting of the sheaths would suppose a perfect thermal conductivity, which is not the case. Therefore it can be assumed that the TC and FBG won't be severely damaged during operations. Finally, the fixation system of the LP is far enough below the surface, and the maximal temperature around it is 900°C.

3. High heat flux test

In order to evaluate the thermomechanical behaviour of the G-PFU and the endurance of , HHF tests have been performed on this inertial component. During these tests, the attachment integrity should be checked to verify that it can tolerate the deformations caused by the temperature field, both during the heating phase (peaked temperature) and after the cooling phase (homogeneous temperature) as shown in the previous section. The tested component was composed of two different types of elements, one was the standard type and the second the larger one (see previous section). Also two prototypes of LP and one TC were installed just under the neutral beam maximal heat flux pattern.

Figure 4: Assembly of the two tested PFU

The following loadings have been completed: 1 pulse at 3.5MW/m² during 5s (Tmax = 620°C), 2 pulses at 3.5MW/m² during 18s (Tmax = 1200°C), 2 pulses at 10.5MW/m² during 3.5s (Tmax = 1600°C) and 1 pulse at 3.5MW/m² during 40s (Tmax = 1600°C). ANSYS simulations were done with parameters similar (heat flux and duration) than those used during the HHF tests. The surface temperature was measured by an infrared pyrometer at GLADIS. It was compared to the temperature computed on Figure 5. For both extreme pulses (3.5MW/m² - 40s and 10MW/m² - 3.5s), the temperature development was well simulated. It confirms that modelling was appropriate to describe this object.

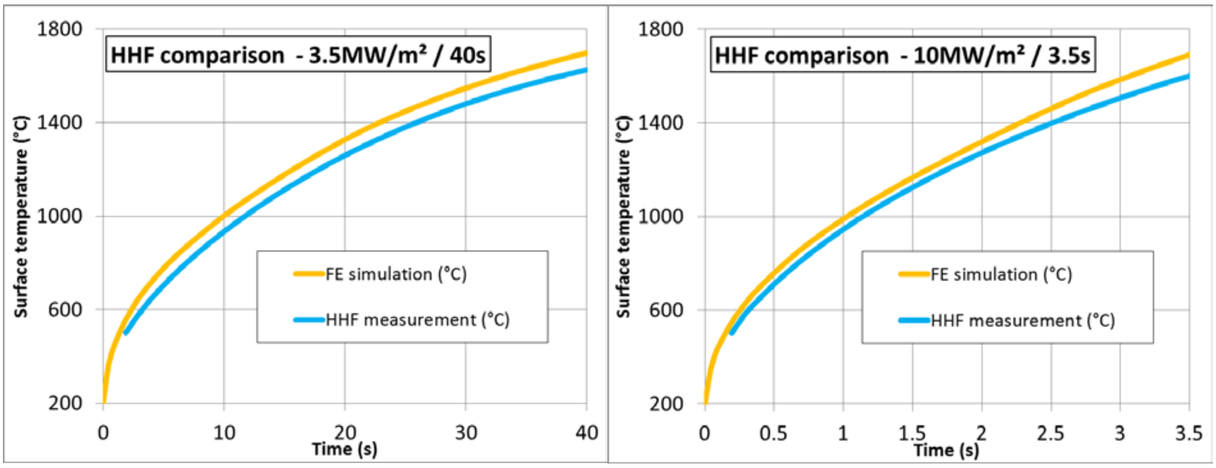

Figure 5: Comparison of the surface temperature measured during HHF tests with ANSYS simulations

The test was positive, as no cracks occurred for the different load cases. In particular, the attachment had proven its ability to sustain the high temperature due to a low heat flux for longer pulse duration. The TC did not break during the test. Contrary to the FEM prediction (section 2.2), the LP inserted in the G-PFU did not survive the HHF test. Indeed, the steel of the screwing support has partially melted, and it was impossible to unscrew. This was unexpected from the previous simulations. Actually two details have been neglected. The first is that the heat flux coming onto the head of the LP is mainly conducted through the LP itself, because LP and G-PFU have poor thermal contact. The second is that some heat flux may be transferred to the LP by thermal radiation between the graphite and the steel surface. Therefore it is plausible that the temperature of the LP was in fact higher than the temperature of the G-PFU, and high enough to melt partially the steel part of the LP.

4. Operational limitations

It can be concluded from the HHF experiment that ANSYS simulations produce valid results in terms of temperature, except for the steel LP diagnostics because of uncertainty in their thermal loads and thermal contact. In order to provide safer margins, and to avoid introducing an operational limit imposed by a diagnostic for the extremely energetic discharge, it has been decided to replace all LP stainless steel components by tantalum.

Therefore, except for this particular diagnostic, it is possible to plot the temperature at the surface and 7.5mm below the surface for different plasma parameters and understand where the limit comes from: either from the coating (l200°C or 1700°C) or from the diagnostic (1000°C to keep some margins to steel melting point). As already said in the first section, the most limiting case, from the thermal point of view, is the one with the maximal heat flux spreading. Therefore the same case is kept: close X-point with a decay length of 5mm. The only varying parameter is the maximal incident heat flux, from 2 to 10 MW/m². The results are shown on figure 6.

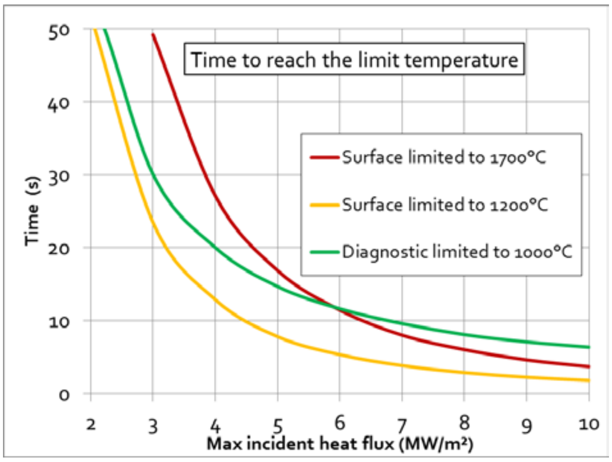

Figure 6: Time to reach the temperature limits for the PFU surface and embedded diagnostics

Obviously the time to reach 1200°C on the surface (yellow curve) is always lower than the time to reach 1700°C (red curve). First observation is that the PFU is not limited by the steel diagnostic (green curve) if the surface temperature is kept under 1200°C, which is the temperature of the W carbidisation. However, if the surface is allowed to go up to 1700°C, the diagnostics may become more limiting than the W coating. Indeed the maximal temperature is reached on the diagnostics before the surface reaches its own limit for incident heat flux lower than 6MW/m². For this kind of plasma parameters, the temperature of the embedded diagnostics should be checked carefully in addition to the surface temperature.

The most challenging part of the WEST project during the early phase of exploitation will be to reach incident heat fluxes of at least 10MW/m² during a time of at least 4s. Indeed during this phase several W-monoblock PFUs will be installed on the lower divertor replacing some of the G PFU. The goal will be to test the W-monoblocks at their nominal operation heat flux (10MW/m²) in order to reach their thermal steady state conditions. Figure 7 shows the time to reach surface temperature of 1200°C (light color) and 1700°C (dark color) for 2 different decay lengths (2.5mm - red curve and 5.0mm - blue curve). The time to reach the limit temperature is given as a function of the power absorbed by the divertor (roughly equals to the injected power minus the radiated power and the power conducted to the others components), while dashed lines give the correspondency between the absorbed power and the maximal incident heat flux onto the surface. The second reference scenario (called far X-point) is also included in this study. Its main characteristic is that the heat flux profile is much more peaked than for the close X-point scenario by a factor of 3. Therefore the area impacted with the highest heat flux is smaller with this scenario.

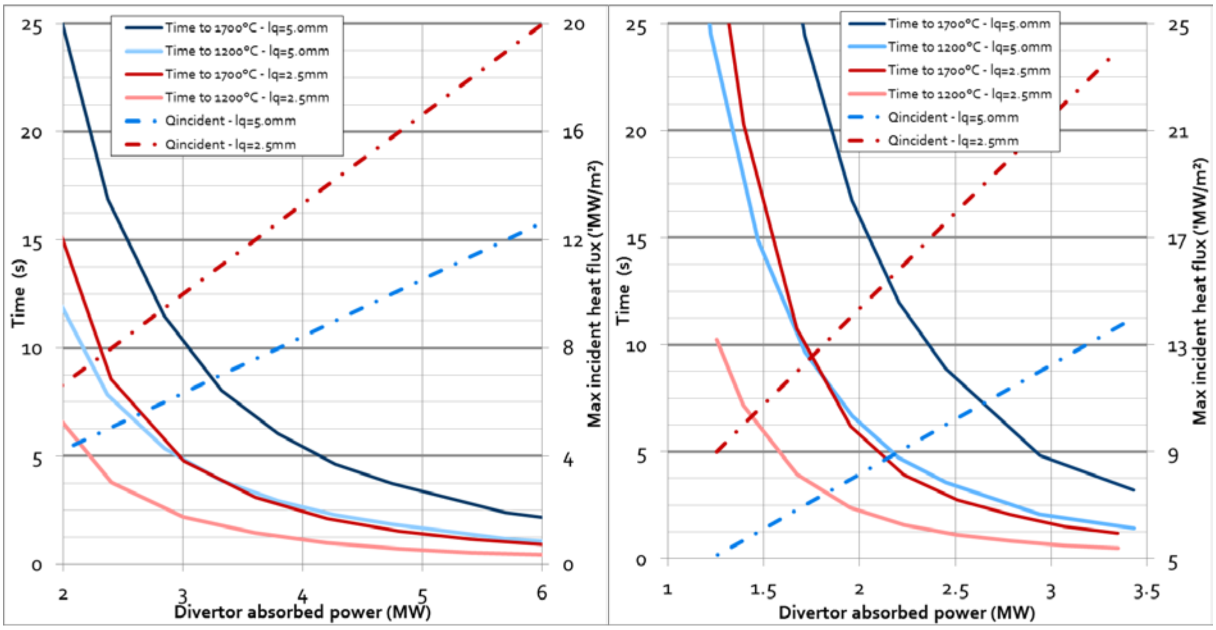

Figure 7: Time limits for the graphite PFU as a function of the divertor absorbed power – close X-point (left) and far X-point (right)

These graphs represent the following result: for 10MW/m² maximal incident heat flux on the G-PFU surface in the close X-point scenario, the absorbed power is 5MW (lq 5mm) or 3MW (lq 2.5mm). For this power, the time to reach 1200°C/1700°C is 1.8s/3.7s (lq 5mm) and 2.2s/4.8s (lq 2.5mm). The main results are summarised in the next table.

(l_q 2.5mm / 5.0mm)	P absorbed (MW)	Time to 1200°C (s)	Time to 1700°C (s)
Close X-point	3 / 5	2.2 / 1.8	4.8 / 3.7
Far X-point	1.4 / 2.5	7.2 / 3.6	20.3 / 8.9

Table 2 : Divertor absorbed power and time to reach the limit of 1200°C and 1700°C for two scenarios and two decay lengths (2.5mm / 5.0mm)

It can be concluded from these simulations that it is possible to heat the G-PFU during a time long enough (> 4s) that adjacent W monoblocks PFU reaches its steady state conditions. However, for the close X-point scenario, the temperature limit to be considered has to be 1700°C, while for the far X-point scenario the limit at 1200°C could be considered, enhancing the lifetime of the W coating.

5. Conclusion and perspectives

The results presented in this paper confirm the suitability of the graphite PFU including its attachment geometry for the required heat flux. It is also shown that the stainless steel based diagnostics embedded in some G-PFU should not limit the operation more than the W coating for the challenging part of the WEST research plan (high power plasma). However in the case of low incident heat fluxes (low power plasma), and if the surface is allowed to reach higher temperatures (long duration pulse), the diagnostics will be a limit to check. About the specific case of LP, it has been demonstrated by experiment that the instrumentation can reach higher temperature than expected. Consequently, it has been decided to change the support material of the probes from stainless steel to tantalum which is much more tolerant to high temperatures.

It is also shown that the thermal simulations exhibit a good agreement with the HHF experiment.

Finally, the last section demonstrates that there is a trade-off between the level of flux required (10MW/m² in this paper), the wetted area and the coating lifetime. But in any case, it seems possible to operate at a power so that the maximal incident heat flux on the lower divertor is 10MW/m² during a time longer than the time for the W monoblock PFU to reach its steady-state.

Some work has still to be done, in particular an HHF test on the graphite PFU including the W coating; the expected performances of the coating should be confirmed on the G-PFU itself.

6. References

[1] J. Bucalossi et al., Fusion Engineering and Design 89 (2014) 907-912.
[2] H. Greuner et al., Journal of Nuclear Materials 367–370 (2007) 1444.
[3] M. Firdaouss et al., Fusion Engineering and Design Available online 7 January 2015, ISSN 0920-3796, http://dx.doi.org/10.1016/j.fusengdes.2014.12.024
[4] R. Neu et al., Physica Scripta T138 (2009) 014038
[5] C. Ruset et al., Fusion Engineering and Design 86 (2011) 1677–1680